Control Of Tip-Leakage Flows Using Periodic Excitation

by

Eugene K. Kang

B.S., Mechanical Engineering (1998)

University of California, Berkeley

Submitted to the Department of Aeronautics and Astronautics
in Partial Fulfillment of the Requirements for the Degree of
Master of Science in Aeronautics and Astronautics

at the

Massachusetts Institute of Technology

January 2000

Signature of Author .....
Department of Aeronautics and Astronautics
January 14, 2000

Certified by .....
Kenneth S. Breuer
Visiting Associate Professor of Aeronautics and Astronautics
Thesis Supervisor

Accepted by .....
Nesbitt Hagood
Associate Professor of Aeronautics and Astronautics
Chairman, Department Committee on Graduate Students

Control Of Tip-Leakage Flows Using Periodic Excitation

by

Eugene K. Kang

Submitted to the Department of Aeronautics and Astronautics
on January 14, 2000 in partial fulfillment of the
requirements for the degree of Master of Science in
Aeronautics and Astronautics

ABSTRACT

Many flows can be characterized as leakage flows from high-pressure sides to low-pressure sides, resulting in increased inefficiency. This paper experimentally explores reducing leakage flows using periodic excitation. A synthetic jet actuator was used as the periodic excitation source in this experiment. The synthetic jet when excited periodically produces momentum but no net mass flux.

Two speakers were used in these experiments as actuators: a high-frequency compression driver and a low-frequency woofer. The speaker exit cavity was covered with plates leaving only a small rectangular orifice exit for the synthetic jet. An airtight plexiglass box with a small gap was used to create a simulated leakage flow. The synthetic jet was then directed normally into the leakage flow to reduce the effective gap.

The variables considered were as follows: the momentum flux ratio of the actuator over the leakage flow, the reduced frequency, the ratio of the height of the clearance gap over the thickness of the gap, and the ratio of the width of the orifice exit over the thickness of the gap. The ratio of discharge coefficient with actuation over the baseline discharge coefficient was used as the figure of merit.

The results showed that the momentum flux ratio exerted a great influence on the leakage flow. A reduction of nearly 70 % in discharge coefficient ratio was achieved at a momentum flux ratio of 70. The reduced frequency was also found to have a significant effect, with the effectiveness of the actuator decreasing as the reduced frequency increased. The geometric parameters had little effect on the leakage flow.

Thesis Supervisor: Kenneth S. Breuer

Title: Visiting Associate Professor of Aeronautics and Astronautics

Table of Contents

1.0 Introduction

1.1 Overview and Motivation

Leakage flows, defined as undesirable flows escaping from a high-pressure side to a low-pressure side through a small gap, occur in many applications. Examples include leakage in bearings and seals, but the leakage flow most relevant to this paper is the leakage flow in turbomachinery through the clearance gap between the blade and the casing. The tip leakage flow results in a pressure loss and decreased efficiency, but the reduction of leakage by reducing the physical clearance gap is not always desirable nor feasible. Tighter manufacturing tolerances and smaller clearance gaps are not only expensive and present maintenance difficulties, but also are sometimes physically impossible to achieve. Thermal expansion of the blade, for example, sets a physical limit for possible clearance. This paper seeks to present an alternative method of reducing the leakage flow using periodic excitation, which would reduce the losses and inefficiencies but without imposing stricter mechanical tolerances.

The method of leakage flow reduction using periodic excitation centers around the utilization of the synthetic jet actuator. A synthetic jet, when excited periodically, produces no net mass flux but provides a momentum source. A schematic of the synthetic jet actuation scheme is presented below in Figure 1.

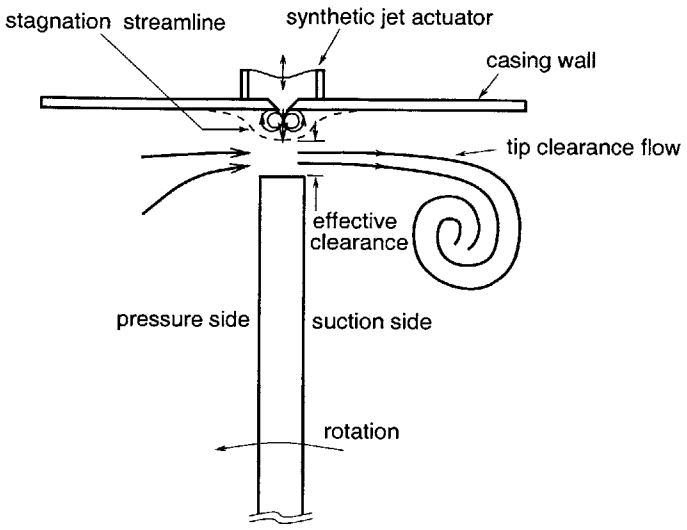

Figure 1. Schematic of actuation scheme to reduce effective tip clearance.

The synthetic jet, by injecting momentum normal to the leakage flow, can help reduce the effective gap by shifting the stagnation streamline and creating a virtual surface. It is a concept analogous to that of the air curtain (used widely for temperature control in doorways and such), with the major difference being that the air curtain relies on mass injection to block incoming flow whereas the synthetic jet relies on momentum injection. This scheme has a couple of major advantages. For one, issues relating to mass injection can be avoided (such as the necessity for piping or tubing and punps), since there is no net mass flux. Also, the synthetic jet can be placed on the casing instead of on the blade itself, reducing the complexity of installation and maintenance.

The motivation for this work, then, is to prove that the concept of synthetic jet actuation can be used to reduce leakage flow and losses associated with it; furthermore, optimum conditions for effectiveness will be explored.

1.2 The Synthetic Jet

Much of the credit for the popularization of the synthetic jet is due to Ingard, who studied acoustic cavity resonators in the 1950s, and Glezer in particular, who has coined the term "synthetic jet" and who has made great use of the device in fluidic control [1]. A schematic of the synthetic jet actuator used in this experiment is shown below in Figure 2.

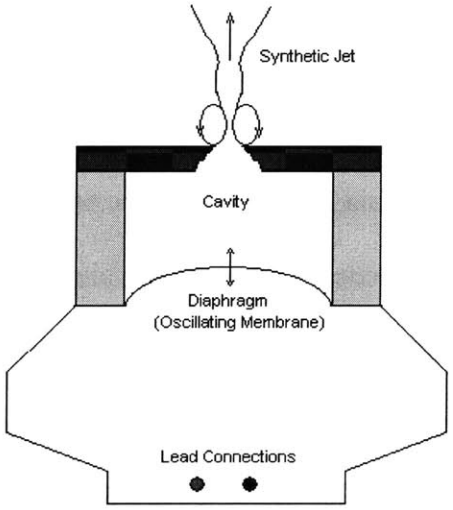

Figure 2. Schematic of synthetic jet actuator.

In the synthetic jet shown above, the membrane represents an end wall of the cavity and the opposite end wall has a small orifice exit. The membrane can be thought of as a piston; on the upstroke of the membrane, it compresses the fluid and pushes it out of the cavity through the orifice exit in the form of a jet normal to the exit plane. On the downstroke of the membrane, the membrane sucks fluid in from all around the near-field of the orifice exit. This results in a zero mean velocity through the orifice exit and therefore in a zero net mass flux.

One of the most important characteristics of the synthetic jet is the distance downstream to which the periodic effect of the oscillating membrane can be felt. Smith and Glezer [1] have determined that the periodicity of the phase-averaged centerline velocity depends on the non-dimensional lengthscale defined by the x-distance downstream divided by the width of the orifice exit (for a rectangular slot orifice exit shape). When this dimension (referred to as x/h by Smith and Glezer) is zero (i.e., right at the orifice exit), the phase-averaged velocity over one cycle strongly resembles a sinusoidal wave, meaning that the suction velocity created by the downstroke of the actuator is the same magnitude as the jet velocity created on the upstroke. At $x/h = 3$, the effect of the suction stroke is not felt anymore; that is, there is no noticeable "negative" velocity on the downstroke of the actuator, only a positive velocity out of the cavity on the upstroke. At $x/h = 9.8$, there is almost no noticeable periodic effect at all; in other words, at this distance a steady non-periodic jet is seen. This can effectively be described as the far-field, then, whereas the region in which $x/h < 9.8$ can be described as the near-field. This division is important because it affects the method in which the velocity is measured. In the far-field, a time-averaged velocity will suffice, since there is no periodic variation in velocity that far downstream. In the near-field, however, there *is* a sinusoidal form to the phase-averaged velocity, meaning that a time-averaged velocity may not be the appropriate velocity to measure. Most of this experiment was run in the near-field, and the velocity chosen to represent the synthetic jet was the peak phase-averaged velocity. This will be discussed in greater detail in Section 2.3.

Another important feature of the actuator depicted above is the acoustic cavity. The associated Helmholtz resonance frequency depends only on the geometry of the

cavity and the orifice exit. The resonance can be exploited by actuating at the Helmholtz frequency, resulting in a greater jet velocity than if it were to be actuated at a different frequency.

Ingard's pioneering work characterized the nature of the jets produced by acoustic cavity resonators. He describes four possible "phases" or states that the flow out of an orifice can have; these regions are generally progressed through in order from one to four as the velocity of the flow increases [2]. He describes the first and second regions as low intensity steady regions with vortices around the orifice edges; they differ only in the direction of the flow along the axis. Phase three is of slightly higher intensity, and in addition to the vortices periodic effects can be seen. Phase four is a high intensity region with a fully formed periodic jet. While flow visualization was not done to determine the region and nature of the orifice exit flow in this experiment, it is reasonable to assume that the flow was indeed a fully formed jet, since it exhibited pulsating behavior and strong amplitudes.

In this experiment, the synthetic jet is driven by a speaker, which in turn is driven by a sinusoidal voltage input. A speaker consists, of course, of a cavity and an oscillating membrane which generates pressure waves, which is exactly the acoustic cavity resonator referred to above.

1.3 The Air Curtain Principle

A brief word should be said about the air curtain principle, although again it must be stressed that the air curtain relies on mass injection to achieve its effect while the

scheme proposed in this paper utilizing synthetic jets relies on momentum injection. However, the principle is simple and the analogy useful in understanding the gap blockage scheme.

The air curtain is widely used in industrial and commercial applications to prevent outside airflow from entering a building. As Abramovich relates [3], it is a simple principle: jets of air flow out of slots placed underneath the door and at an angle into the oncoming flow (assumed to be horizontal). The inclined jets intercept the oncoming flow and deflect the flow upwards. If the amplitude of the jets is high enough and the angle is selected properly, then the jets will deflect the flow upwards enough so that the oncoming flow will hit the physical wall above the door. This results in no inflow into the door from outside, effectively blocking off the door with an air curtain.

Abramovich also determined the angle of inclination necessary for the maximum range, which is the maximum height that can be completely blocked off. The key assumption in the analysis is that the vertical component of the jet velocity is not affected by the oncoming horizontal flow, while the horizontal component is added to the oncoming flow. The end result is that the optimum angle is approximately 36° from the horizontal into the flow.

Unfortunately, in this experiment, it was not physically possible to alter the angle at which the synthetic jet was directed. The jet direction was fixed so as to always inject momentum normal to the oncoming leakage flow. This is less than ideal, but could not be helped.

2.0 Experimental Description

2.1 Physical Configuration

A simple experimental configuration, shown in Figure 3, is used to evaluate control performance.

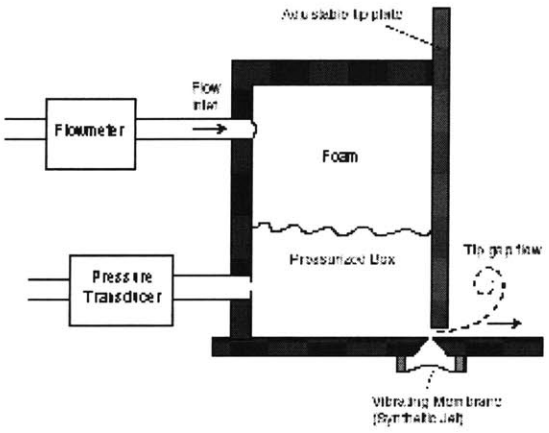

Figure 3. Schematic of experimental setup for actuated tip flow. Both the gap height and the location of the actuator with respect to the gap can be varied.

The experiment consists of two major components – a pressurized box and a baseplate that sits on top of the actuator and creates the actuator exit orifice. The pressurized box has an adjustable faceplate that can move up and down in the vertical direction so as to allow for variation in the height of the gap. The baseplate sits on top of the actuator. For this experiment two different actuators were used: one high frequency compression driver, and one low frequency speaker. An adjustable gap provides the sharp-edged actuator exit orifice. The flow enters the box from the inlet in the upper left side of the

box and then escapes through the gap. The synthetic jet actuator injects a flow normal to the leakage flow at a specified amplitude and frequency.

Two actuators were used. The higher frequencies were handled by a JBL Professional Series Model No. 2446J compression driver. The low frequency speaker used was a Radio Shack Realistic Model 40-1024 speaker. The JBL driver was driven from 500 to 2500 Hz with sinusoidal inputs from a Stanford Research Systems DS345 function generator via a Yorkville AP4040 amplifier at post-amplification voltages of 0.5 to 10 V amplitude. The Radio Shack speaker was driven with the same voltage range but at frequencies from 10 to 600 Hz.

The dimensions of the box were 4 inches wide by 5 5/8 inches long by 10 inches high, with the walls being 3/8 of an inch thick. Three faceplates for the box were made: two that were 3/16 of an inch thick and 11 inches tall, and one that was 3/8 of an inch thick and 11 inches high. Each faceplate was fitted with six slots (three on the left side and three on the right) which lined up with holes drilled in the walls of the box so that the faceplate could be moved up and down, creating a variable leakage flow gap. The plate was held on to the box by screws. The box was fed with air from the back near the top of the box, and the upper half of the box was filled with foam so as to slow down and stagnate the supply flow before making its way down to the bottom half of the box and then escaping through the gap. A pressure tap was drilled in the back of the box near the bottom, and this is the pressure that was measured for the final data.

The baseplate was built in two pieces so as to be able to create a variable actuator orifice exit. The stationary part was 8 inches long and 7 inches wide, with a thickness of 1/8 of an inch. The edge that sat over the center of the actuator (where the orifice is) was

beveled to create a knife-edge. This part was screwed into the actuator structure and was not permitted to move. The other piece, which was dimensioned at 4 inches long, 7 inches wide, and 1/8 of an inch thick with the same beveled edge, was given slots to allow the piece to shifted laterally and create an orifice exit of variable width. This piece was also attached by screws, once the desired orifice exit width was set. The orifice exit width was set by using 1 mm pieces of shim stock to separate the pieces, as was the leakage flow gap.

2.2 Discussion of Parameter Choice

In this configuration, six non-dimensional parameters were used to describe the experiment: amplitude ratio of the actuator over the leakage flow (measured in momentum flux), reduced frequency, Reynolds number, and three non-dimensional geometric parameters relating the area of the tip clearance, the area of the actuator orifice exit, and the location of the actuator relative to the thickness of the tip. The change in discharge coefficient, defined as the actual flow rate divided by the ideal flowrate) was chosen as an appropriate measure of effectiveness, as discussed below. A list of non-dimensional parameters and definitions follows below:

Amplitude ratio: $$\frac{momentum\ flux_{actuator}}{momentum\ flux_{leakage\ flow}}$$

Reduced frequency: $$\frac{2\pi f \times blade\ thickness}{velocity_{leakage\ flow}}$$

Gap aspect ratio: $\frac{tip\ clearance\ height}{blade\ thickness}$

Actuator gap ratio: $\frac{actuator\ exit\ width}{blade\ thickness}$

Actuator location: $\frac{actuator\ x-location}{blade\ thickness}$

Gap Reynolds Number: $\frac{velocity_{leakage\ flow} \times gap\ height}{vis\cos ity}$

A word needs to be said about the selection of the amplitude ratio. There were two possibilities considered to characterize the amplitude of the synthetic jet - velocity and momentum flux. In the final analysis, momentum flux ratio was selected as an appropriate measure of amplitude ratio. Initially, preliminary experiments were run with both measures in mind; however, as will be discussed in the results section in 3.1, the preliminary results indicated that momentum flux was a more relevant parameter.

Before final experiments could be run, however, it was desirable to further reduce the number of non-dimensional parameters to be explored, if at all possible. The first parameter considered was the Reynolds number. According to a loss factor analysis based on Idel'chik's work [4], it was determined that for the geometry of the experimental setup, the baseline discharge coefficient varied slightly (from about 0.62 to 0.68) for the range of Reynolds numbers and physical geometric parameters covered in the experiments. The measured variation ranged from 0.66 to 0.71. This small variation was deemed acceptable and the leakage flow was considered to have only a weak dependence on the Reynolds number in these experiments. Consequently, experiments were not run

with the Reynolds number in mind as a parameter, and as a result this paper is inconclusive as far as the effects of the Reynolds number are concerned.

The non-dimensional parameter completely eliminated was the x-location of the actuator relative to the front plate. Preliminary tests were run to determine the effect of the actuator location, and it was clearly evident from the results that the optimum location for the actuator was directly underneath the midway point of the thickness of the plate. For all subsequent experiments the actuator was placed there and the x-location was not treated as a variable, as the primary interest lies in maximizing the effectiveness of the actuator.

That leaves, then, only four non-dimensional parameters as experimental variables. The momentum flux ratio was varied from 0 to 80 while the reduced frequency was varied from 0 to 30. The geometric parameter describing the gap aspect ratio was varied from 0 to 1, based on the fact that a real compressor will have an aspect ratio of about 1 and a real turbine will have an aspect ratio of about 0.3. The geometric parameter relating the orifice exit width to the plate thickness was varied from 0 to 0.25. Having no current real-life counterpart, it was originally desired to increase this parameter at least to a value of 1 and beyond, but due to calibration limitations this was not done. Most of the experiments were run attempting to hold three of the four variable constant while the fourth was varied, although in some cases it was either not possible or desirable.

The other variable which may be of importance but was not considered is the angle at which the synthetic jet meets the leakage flow. Due to physical limitations of the system, the jet was directed only in the normal direction, whereas, as mentioned before,

the jet may be more effective at blocking the leakage flow when directed at an angle into the oncoming flow.

2.3 Experimental Procedure

The first step was to calibrate the hot-wire probe. The calibration setup is shown below in Figure 4.

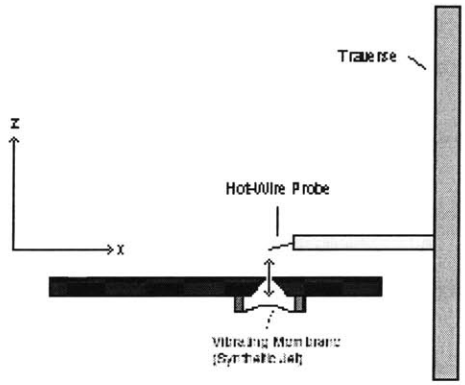

Figure 4. Schematic of calibration set-up.

The velocity profiles were taken in the x-direction, or horizontally in the diagram above. When the hot-wire was measuring in the "negative" x-region, the probe itself was located directly above the orifice exit and interfering with the synthetic jet. For this reason only half-profiles were taken and symmetry was used to complete the profile. Ideally, full profiles would be taken but that was not possible here.

It should also be noted here that the hot-wire could only be calibrated to velocities of approximately 30 m/s, due to the velocity limitation of the wind tunnel which was used to calibrate the hot-wire. A sample calibration is shown below in Figure 5.

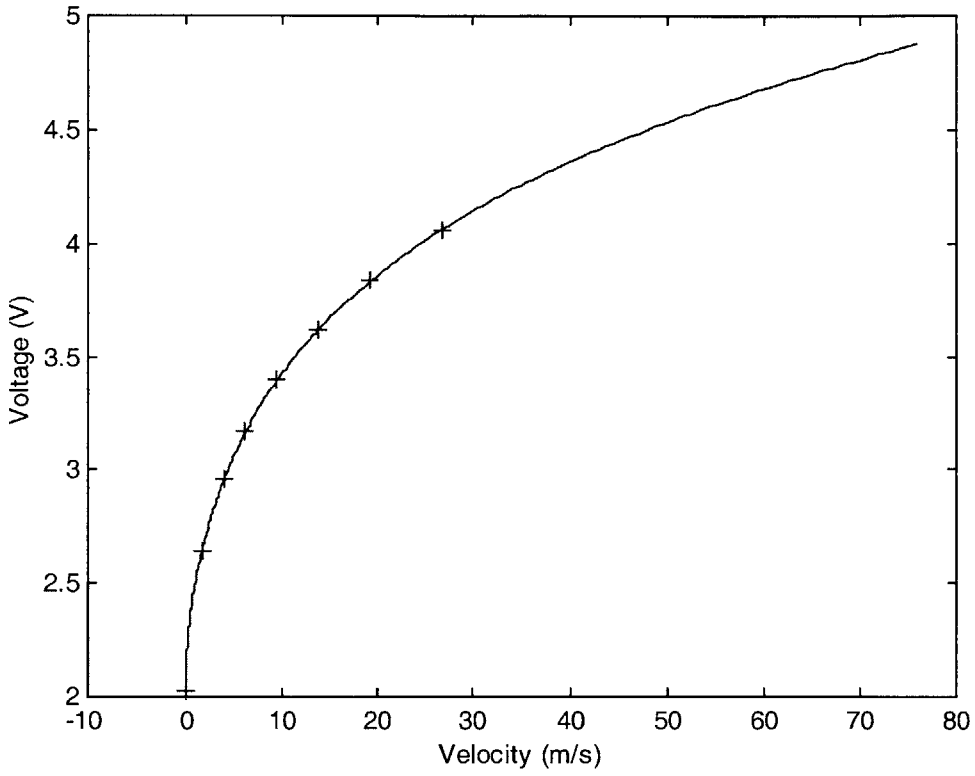

Figure 5. Sample calibration curve for hot-wire calibration in the wind tunnel.

In Figure 5, the calibration is extrapolated as far out as almost 80 m/s; in this experiment, the synthetic jet was producing close to 50 m/s second, which is still well beyond the last measured velocity in the calibration curve.

In order to obtain the momentum flux of the actuator, a velocity profile of the synthetic jet coming out of the actuator was measured with a hot wire, and then integrated so that

$$momentum\ flux_{actuator} = \iint \rho u^2 dA$$

where the velocity is assumed constant in the y-direction but varies along the x-direction (across the actuator exit slit). A sample velocity profile is shown below in Figure 6.

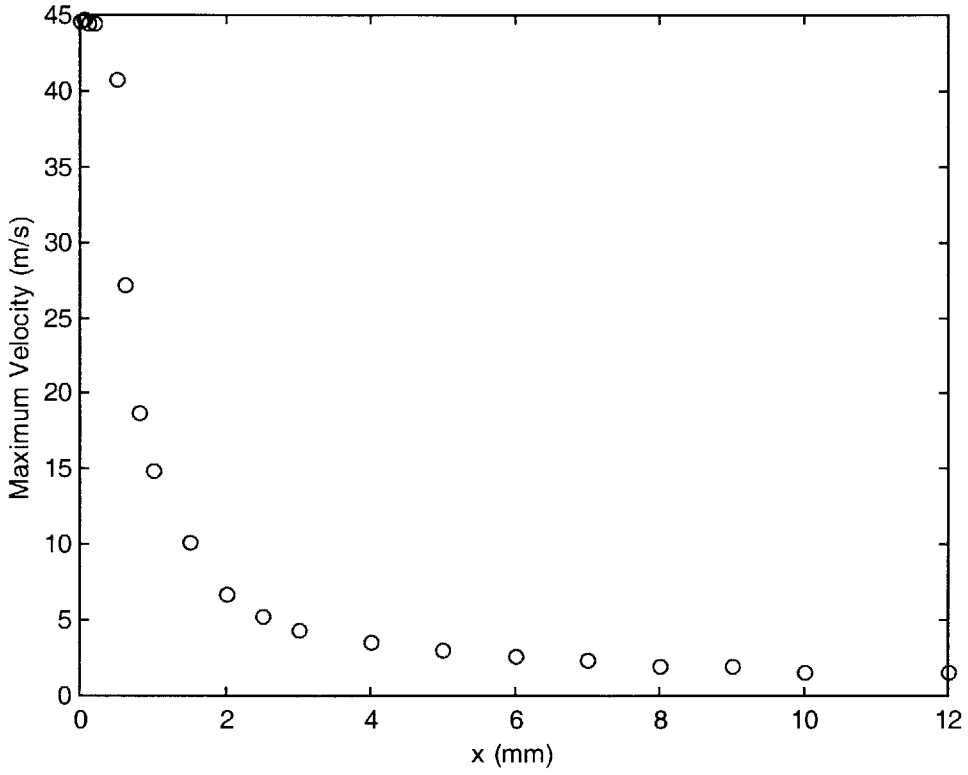

Figure 6. Sample velocity profile. This is for the JBL compression driver, orifice exit of 1mm, voltage of 10 V amplitude, frequency of 500 Hz.

The problem with measuring the momentum flux of the synthetic jet is deciding which velocity to use in defining it. In Figure 7 below is shown a phase-averaged (over 10 cycles) centerline velocity of one cycle of the synthetic jet, at 10 volts amplitude and 500 Hz.

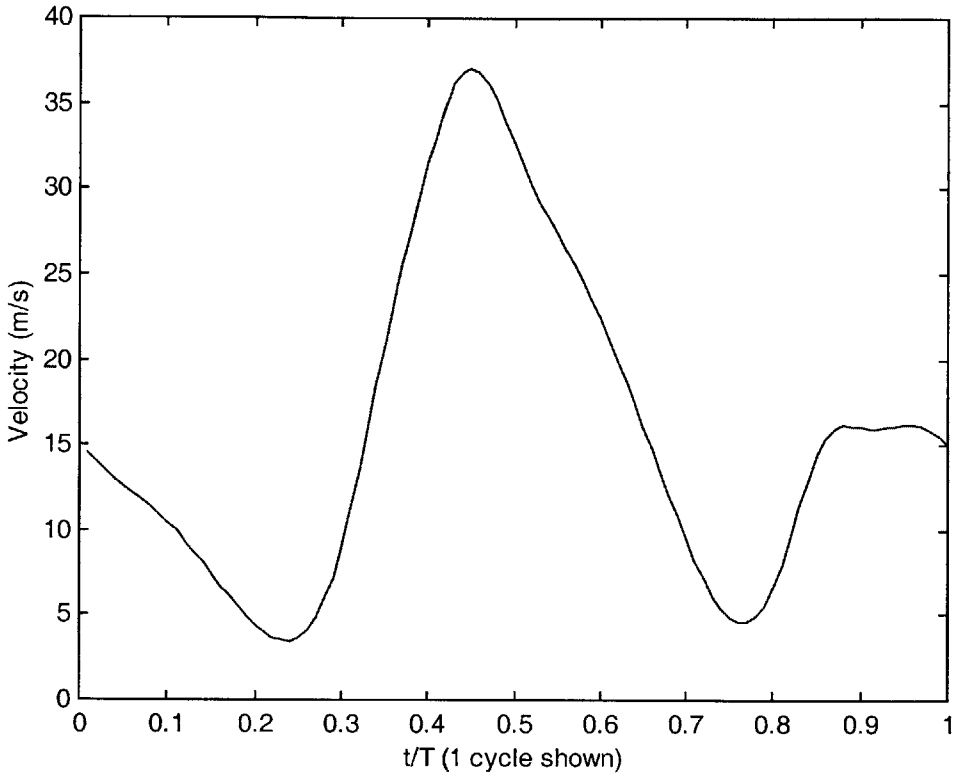

Figure 7. Measured velocity over one period of the synthetic jet.

For these experiments, the velocity chosen to determine the velocity profile and therefore the momentum flux of the synthetic jet was the peak velocity of the phase-averaged cycle, which in Figure 7 above occurs near $t/T = 0.45$. However, this does not accurately represent the time-averaged momentum flux into the leakage flow; rather, it is a measure of *peak* momentum flux into the leakage flow. Since the x/h variable in these experiments varied from 1 to 8, the region of interest could be said to be in the near-field rather than the far-field. As such, the velocity and therefore the momentum flux of the synthetic jet is almost certainly over-estimated in this paper, but is still valid as a relative measure of momentum flux and therefore amplitude.

The other feature of Figure 7 which should be noted is the secondary "peak" composed of the left and right ends of the plot (approximately 15 m/s). This is not really a peak, but the negative portion of the cycle, or the suction portion. Here the actuator is drawing in fluid, but since the hot-wire measures only the magnitude of the velocity and not the direction, the fact that the velocity is now being sucked into the cavity instead of being expelled out is not reflected here. The magnitude is also much lower on the suction stroke since it is drawing fluid in from all around the orifice exit, as opposed to the expulsion stroke where the outgoing fluid is much more strongly focused.

The momentum flux of the leakage flow was calculated by measuring the mass flow, calculating the average flow velocity knowing the area, and then using the above integrated formula such that

$$momentum\ flux_{leakage\ flow} = \rho u^2 A$$

The momentum flux for the profile shown above in Figure 6 is 0.17 kg-m/s^2.

The first step in the procedure, then, was to calibrate the two actuators at various input amplitudes and frequencies, so that no matter what input into the actuator the exit velocity and momentum flux were known. As mentioned above, this was done using a hot-wire traverse system. The actuators were driven by a sinusoidal input from a function generator via a power amplifier, with amplitudes ranging from 0.5 volts to 10 volts and frequencies from 500 to 2500 Hz for the compression driver and from 10 to 600 Hz for the low frequency speaker. Profiles were taken at discrete voltage and frequency intervals, usually one volt intervals and 50 to 100 Hz intervals. Points in between those

actually measured were interpolated from the framing data. An example of an interpolated synthetic jet calibration is shown below in Figure 8.

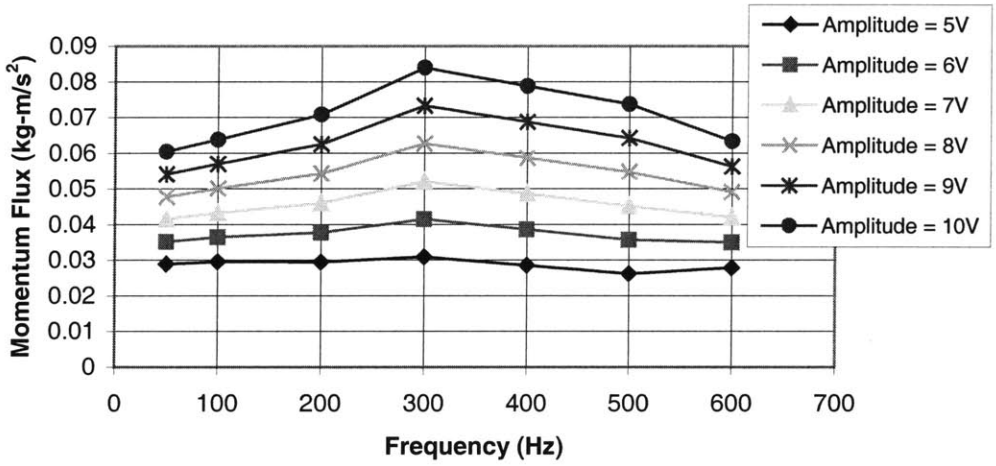

Figure 8. Interpolated actuator calibration for Radio Shack speaker, orifice exit width of 1mm. Symbols represent measured data points and lines represent the interpolation.

For any voltage and frequency input within the desired range to the Radio Shack speaker with an orifice exit width of 1mm, the output momentum flux can be determined using the plot above. Note that at low amplitudes the response is fairly constant with frequency, but peaks at around 300 Hz at higher amplitudes.

In Figure 9 below is shown the transfer function for the JBL compression driver for constant amplitudes of 10 V and 2.5 V.

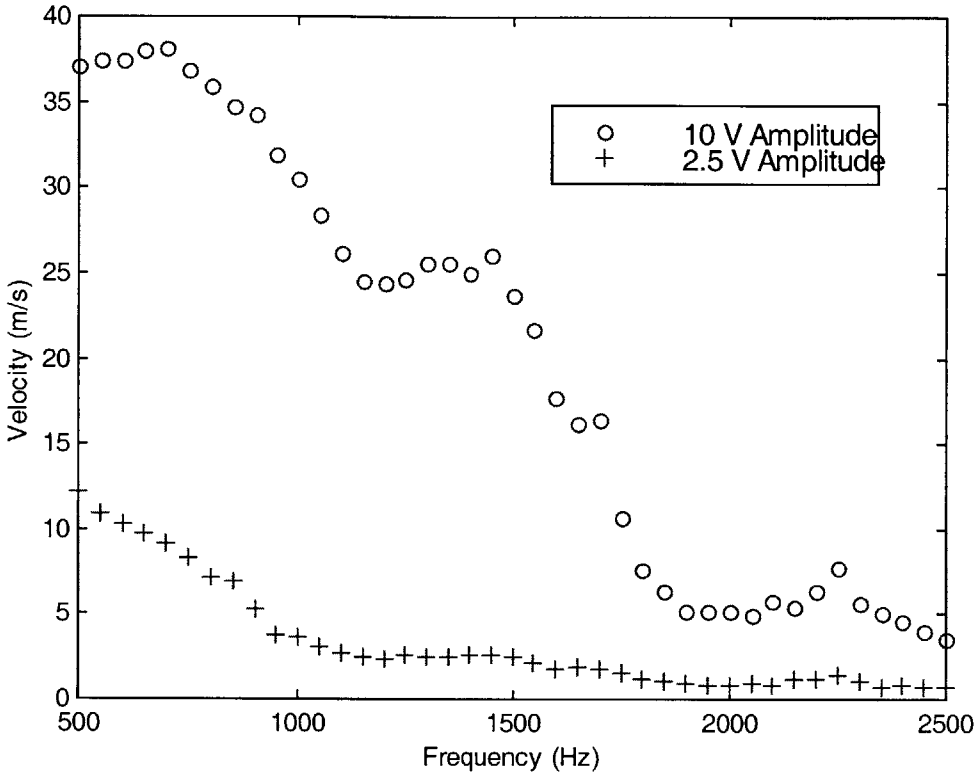

Figure 9. Transfer function for JBL compression driver at 10 V and 2.5 V amplitudes.

The transfer function for the JBL compression driver reveals a couple of interesting things. First of all, performance decreases as frequency increases, which is expected. More interestingly, though, there are three peaks - one at 750 Hz, one at 1500 Hz and one at 2250 Hz. The even intervals of 750 Hz suggest a harmonic phenomenon of sorts, perhaps a mechanical resonance. The calculated Helmholtz resonance frequency for this speaker and cavity was about 2800 Hz, which may be the sharp peak observed at 2250 Hz. Also, and increase in amplitude by a factor of four does not necessarily result in an increase in velocity by the same factor. At 500 Hz, the velocity at 2.5 V is actually one-third that of the velocity at 10 V rather than a quarter. However, at higher frequencies,

the actuator produces a very low velocity at 2.5 V, and hardly reflects the peaks clearly visible at 10 V amplitude.

After calibration, the actuator was then placed into the setup described previously and depicted in Figure 3 previously. The leakage flow, supplied by a Speedaire air compressor, was turned on and allowed to settle down before the mass flow and pressure in the box were measured. The mass flowrate was measured using a Hastings Model HFM-201 flowmeter, which has a range of 0 to 300 SLPM with an accuracy of ±1%. The pressure was measured via an AutoTran Model No. 700D1"24V4 pressure transducer, which has a range of 0 to 1 inch of water. Both the pressure and the mass flowrate, when given time to settle (twenty seconds), provided a stable DC signal. The sampling frequency for both the pressure and flowrate was set at 10000 Hz, with 10000 points being taken per record. The signals for pressure and flowrate were very stable and DC when observed on both an oscilloscope and voltmeter, so the sampling rate and number of points taken were deemed more than sufficient. The actuator was then turned on with the desired amplitude and frequency, and again the mass flow and pressure were measured. The discharge coefficient was determined by dividing the measured flow rate by the ideal flow rate, where the ideal flow rate was based on the area times the ideal velocity

$$u_{ideal} = \sqrt{\frac{2\Delta p}{\rho}}$$

calculated from the measured pressure drop across the gap. The baseline coefficient refers to the case without actuation. The measure of effectiveness is presented as a discharge coefficient ratio, which is the measured discharge coefficient with actuation

divided by the baseline discharge coefficient. This means that zero effectiveness corresponds to a value of one for the discharge coefficient ratio and complete gap blockage corresponds to a discharge coefficient ratio of zero.

The data can also be presented as a percent reduction in the effective gap. The effective gap can be thought of as the gap that the leakage flow sees, whether the gap boundary is defined physically or virtually by the actuator. In the baseline case of no actuation, the effective gap is the same as the physical gap. However, with actuation, the effective gap is smaller than the physical gap, since the synthetic jet will create a barrier that the leakage flow cannot penetrate and will go around. This effective gap is backed out in the following manner: the pressure rise in the box with actuation is recorded, as in the discharge coefficient data reduction. From this pressure an ideal velocity is backed out. This velocity is then multiplied by the baseline discharge coefficient to account for unavoidable orifice losses through the gap; this produces an "effective velocity," if you will. This effective velocity represents the velocity at which the leakage flow should be leaving the gap, based on the above assumptions; unfortunately, this velocity was not confirmed by measurement. Assuming this to be fairly close to the real value, a value for the effective gap can be calculated since the mass flow rate is measured and known.

If the steps to this analysis are actually carried out, however, it can be seen that it is equivalent to carrying out the discharge coefficient analysis. This is to say that the percent reduction in discharge coefficient is exactly the percent reduction in the effective gap. The reduction in the effective gap is actually a useful way of looking at the data, as it presents a more readily identifiable and physical characterization of the effectiveness then the reduction of the discharge coefficient as a metric. It also provides a context with

which to realize concrete improvements in the system; for instance, an effective gap reduction of fifty percent means that if a clearance gap of 2 mm is desired, a physical gap of 4 mm can be physically manufactured, leading to manufacturing cost savings and so forth.

3.0 Results and Discussion

Before any quantitative experiments were conducted, flow visualization was done as a proof-of-concept. With the success of those experiments, the quantitative experiments were then done. The qualitative results are presented first, followed by the quantitative results.

3.1 Qualitative Visual Results

Flow visualization was carried out to verify that the concept of leakage flow blockage using synthetic jets was indeed achievable. Smoke was injected from the rear into the pressurized box and allowed to flow freely through the gap. The left-hand-side photo in Figure 10 below shows the smoke clearing flowing through. When the actuator is turned on, however, the smoke is prevented from flowing through the gap and very little smoke can be seen escaping. This is shown in the right-hand-side photo. The effect is very dramatic, but although this sort of near-complete blockage is obviously possible, these photographs were taken at a very high actuator-to-flow amplitude ratio (estimated to be in excess of 100 with amplitude defined by momentum flux).

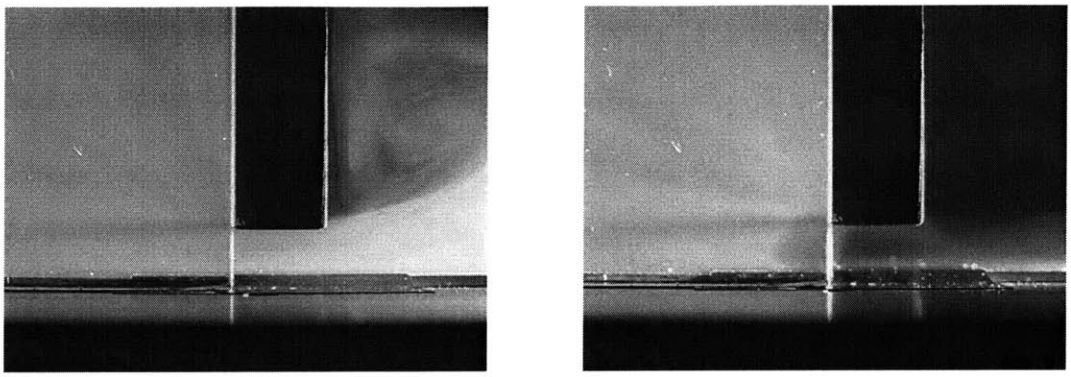

Figure 10. Photographs of tip flow visualized using smoke particles. The left frame shows the flow paths without control. The right frame shows the flow patterns with the actuator aligned with the leading edge of the tip and operating.

Again, it should be emphasized that these were done at high momentum flux ratios, and may not be within the numerical parameters of the quantitative data that follows.

3.2 Selection of Amplitude Ratio

The question of whether to use velocity ratio or momentum flux ratio as a measured of amplitude was settled using the following results. Figure 11 below shows a plot of discharge coefficient ratio vs. momentum flux ratio for two different orifice exit ratios.

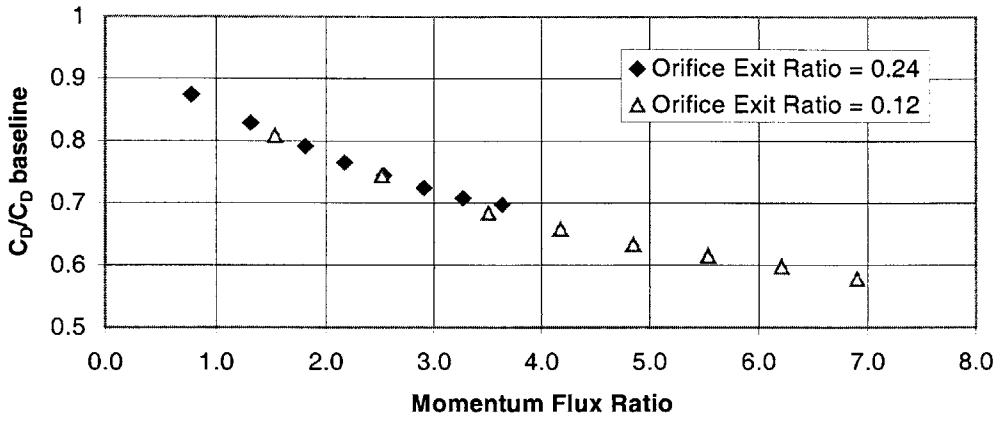

Figure 11. Discharge coefficient ratio vs. momentum flux ratio for two different orifice exit ratios.

The key feature of the above figure is the near-exact overlap of data for different orifice exit ratios. This means that although two different geometrical configurations are used to produce the same momentum flux ratio, the end result is the same. Compare this with the same data plotted below versus velocity ratio in Figure 12.

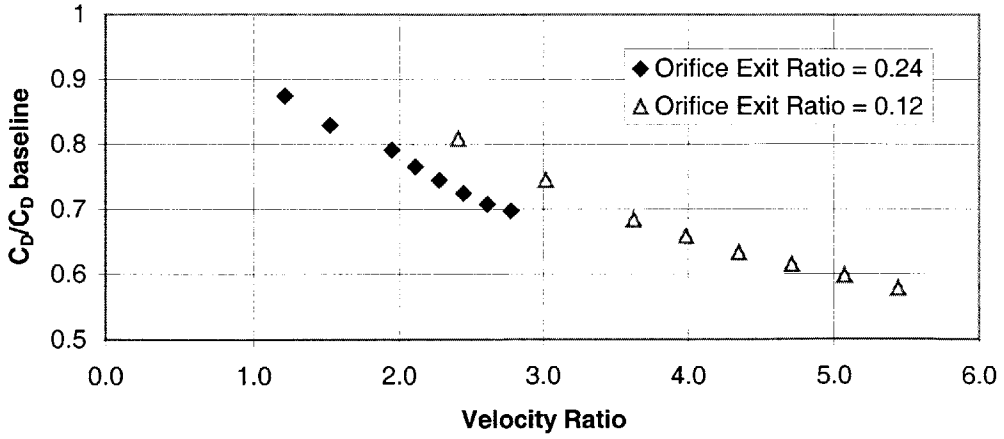

Figure 12. Discharge coefficient ratio vs. velocity ratio for two different orifice exit ratios.

In Figure 12, the data does not overlap when plotted versus velocity ratio. Again, it has to be emphasized that this is the same run as Figure 11, only plotted versus velocity ratio instead of momentum flux ratio. The overlap of data in Figure 11 versus Figure 12 is a good indication that the momentum flux ratio is the proper measure of amplitude. It should also be noted that the small difference in orifice exit ratios is not expected the otherwise impact the results since the exit ratios are small to begin with.

There is also additional evidence to support this choice. In Figures 13 and 14 below are shown two plots of discharge coefficient ratio vs. amplitude ratio for five different aspect ratios. Figure 13 uses velocity ratio as a measure of amplitude and Figure 14 uses momentum flux ratio as a measure of amplitude.

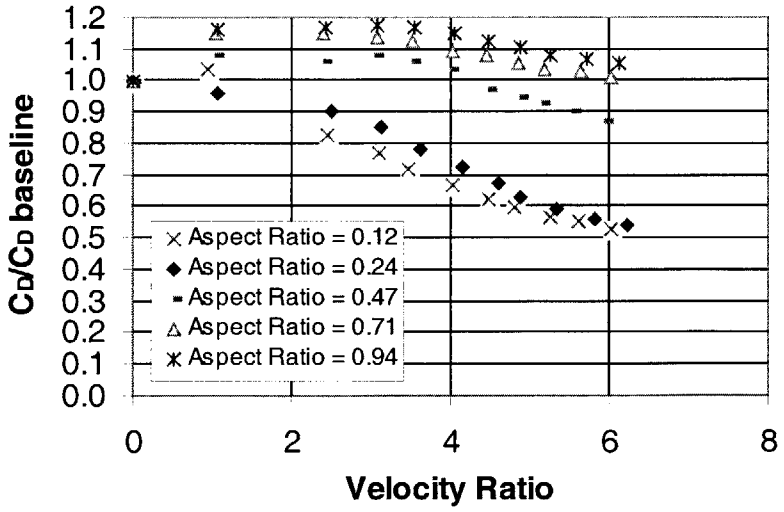

Figure 13. Discharge coefficient ratio vs. velocity ratio.

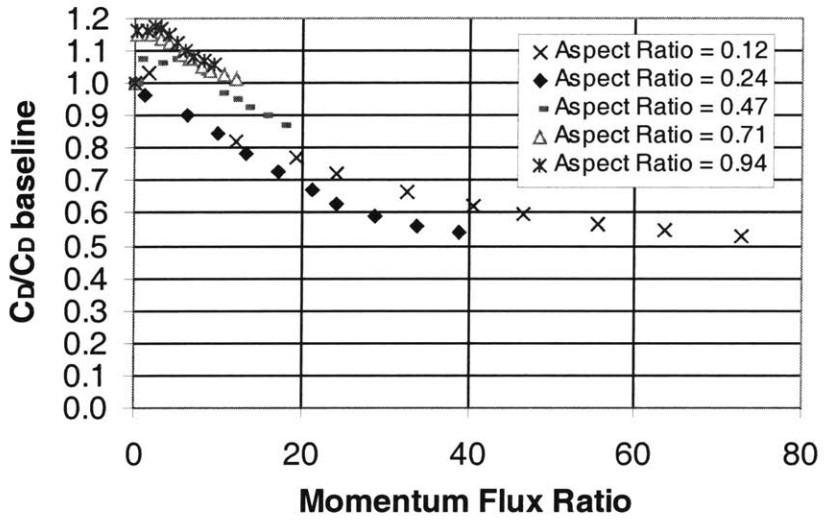

Figure 14. Discharge coefficient ratio vs. momentum flux ratio.

The important feature of Figures 13 and 14 is that the plots show the exact same data; only that the x-axis has been changed to represent the two possibilities for amplitude ratio, as in Figures 11 and 12. Again, the momentum flux plot in Figure 14 is more encouraging. Note that the slope of the reduction in discharge coefficient ratio with increasing amplitude ratio remains constant for the five different geometries when plotted versus momentum flux ratio, but does not do so when plotted versus velocity ratio. In essence, the momentum flux ratio data collapses much better than the velocity ratio data. Because amplitude ratio is likely to be the most dominant variable in the scheme, it is expected that the "slope of effectiveness" alluded to above would not change drastically simply due to the variation of geometric parameters. This is indeed the case when momentum flux ratio is selected as the measure of amplitude.

The other key feature of Figures 13 and 14 is the *increase* in discharge coefficient ratio at low momentum flux ratios. This means that the pressure loss with low actuation

is actually greater than if there were no actuation at all! The reason for this phenomenon is not clear. This only occurs under certain conditions, always at low momentum flux ratios, but not always - the conditions for this event have not been isolated and identified yet. Whether this phenomenon is physical or is a product of measurement has not been determined - however, the author is convinced that it is not a measurement error. This increase in discharge coefficient has been observed on countless occasions in this experimental rig by the author in both preliminary and final experiments, and also has been observed by a colleague in a separate experimental setup. Ultimately, though, as the goal of this experiment was to decrease the discharge coefficient ratio and increase effectiveness, this phenomenon was not explored further.

3.3 Effects of Momentum Flux Ratio

Armed with the validity of the concept, the next step was to quantify the effectiveness of the gap blockage scheme. As discussed before, the measure of effectiveness adopted was the discharge coefficient ratio.

The momentum flux ratio by itself exhibits a significant amount of control on the leakage flow. The effect of the ratio for a given geometry and reduced frequency is shown below in Figure 15.

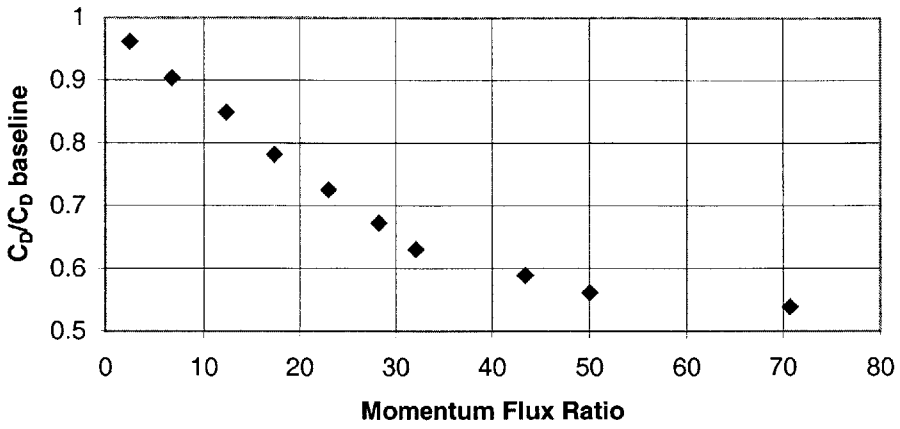

Figure 15. Discharge coefficient ratio vs. momentum flux ratio. This plot was generated at a reduced frequency of 6.

The dependency of the percent reduction in discharge coefficient on the momentum flux ratio is fairly linear at low ratios, increasing steadily as the momentum flux ratio increases. At higher ratios, the effectiveness begins to tail off proportionally to the log of the ratio.

It can also be seen in the figure above that nearly a fifty percent reduction in the discharge coefficient is possible, which is tantamount to a fifty percent reduction in the effective gap. Note that this is achieved at a reduced frequency of six; as will be discussed below, better performance can be gained at lower reduced frequencies. Still, the above plot requires an actuator output that is somewhere from fifty to seventy times that of the leakage flow, which may or may not be feasible in practical applications. Even to achieve a discharge coefficient reduction of twenty-five percent requires a momentum flux ratio of twenty under these conditions. Given the desire to make the actuators small and to reduce power consumption, even momentum flux ratios of five

would be considered large, let alone in the twenty to eighty range. We desire effective actuation but at lower momentum flux ratios.

3.4 Effects of Reduced Frequency

Fortunately, the other important parameter, reduced frequency, can be manipulated in such a way as to achieve better performance at lower momentum flux ratios. Figure 16 below shows a plot of discharge coefficient ratio vs. reduced frequency.

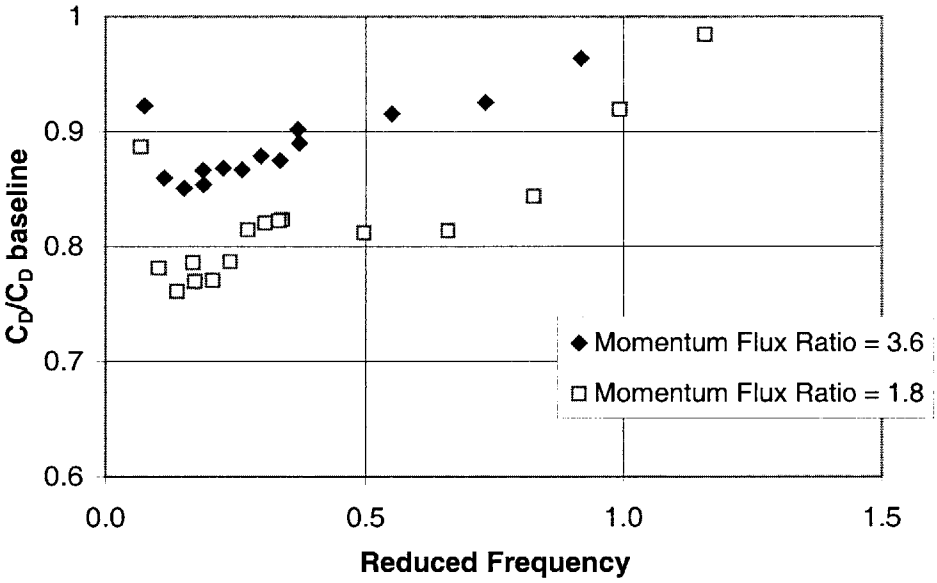

Figure 16. Discharge coefficient ratio vs. reduced frequency for two different momentum flux ratios.

As the reduced frequency is decreased, the actuator becomes more effective, until it reaches a cutoff point at a very low reduced frequency (on the order of 0.1). It can also be seen that there is a peak in effectiveness at around 0.15 for two different momentum flux ratios (1.8 and 3.6). Note that doubling the momentum flux ratio does not quite

double the effectiveness (approximately 2/3 increase in this case). The other phenomenon to note is that the drop-off in performance from peak effectiveness is steep. The range of reduced frequency from peak to zero-effectiveness is only from 0.15 to 1.2. This can be useful in that if the actuator can be operated at the optimum reduced frequency, then the results will be much better than if operated off-peak. However, the down side is that if the optimum frequency cannot be achieved for some reason or if the operating frequency is slightly off, then the system will be much less effective. Also, the optimum reduced frequency changes based on the momentum flux ratio and geometric parameters.

The reason why the actuator works best at low reduced frequencies is simple: the reduced frequency represents, in essence, a ratio of timescales - that of the flow over that of the actuator. When the reduced frequency is high, that means that the it takes the flow much longer to travel through the gap then it does for the synthetic jet to form, be expelled from the orifice exit, and then be sucked back in on the downstroke of the actuator. In other words, the flow does not really "see" the synthetic jet when the reduced frequency is high, thereby reducing the effectiveness of the scheme. Naturally, the improvement in discharge coefficient reduction with the reduction of reduced frequency has a limit; in the extreme, a reduced frequency of zero would translate to no actuation, and obviously this has no effect. Again, the optimum reduced frequency has been found to be on the order of 0.1, but varies based on geometric parameters and also momentum flux ratio. The variation of the optimum reduced frequency with momentum flux ratio is shown below in Figure 17.

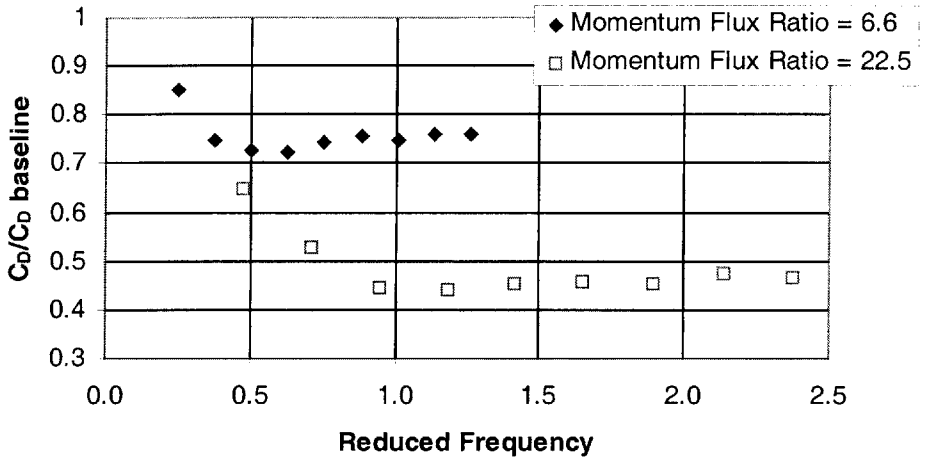

Figure 17. Discharge coefficient ratio vs. reduced frequency for two different momentum flux ratios.

In Figure 17 above, it is apparent that the optimum reduced frequency changes based on the momentum flux ratio. For the lower momentum flux ratio of 6.6, the optimum reduced frequency is about 0.6, whereas for the higher momentum flux ratio of 22.5 the optimum occurs at approximately 1.0. Recall that the optimum reduced frequencies for the momentum flux ratios of 1.8 and 3.6 were around 0.1.

When both the reduced frequency and momentum flux ratio are controlled to maximize effectiveness, a reduction of over seventy percent in discharge coefficient was achieved experimentally. Figure 18 below shows the most effective scheme achieved in this run of experiments.

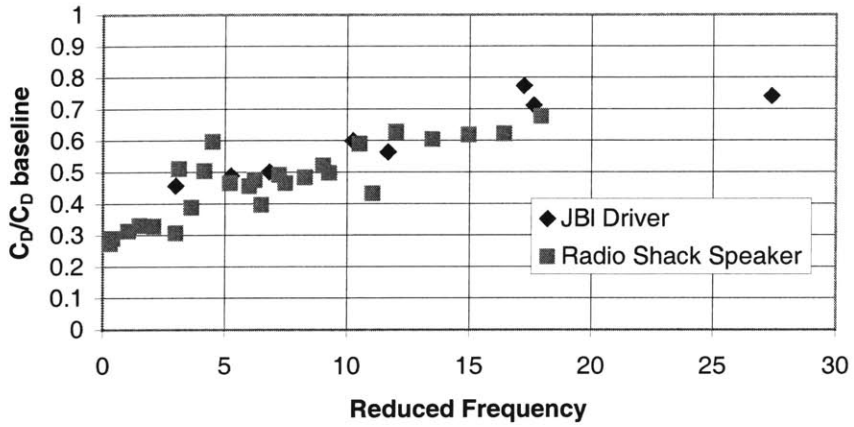

Figure 18. Discharge coefficient ratio vs. reduced frequency. This case is for a momentum flux ratio of 70 and represents the most control obtained in this run of experiments.

In Figure 18, the actuator is driven at a momentum flux ratio of about seventy, and the reduced frequency ranges from 0.5 to almost thirty. The optimum reduced frequency is actually not achieved here, but it is unlikely that a small reduction in reduced frequency to reach that point would significantly impact the effectiveness at this high of a momentum flux ratio. As stated before, this plot represents the most effective scheme achieved during these runs of experiments, although it must be emphasized again that is most likely an unrealistic scenario due to the high momentum flux ratio. The other noteworthy aspect of this plot is the relative overlap of data points gathered using two different actuators. While there is some scatter, the results here appear to be fairly good, considering all of the uncertainties in calibration, physical setup, and measurement. This further confirms the validity of reduced frequency as an important non-dimensional parameter in the characterization of the gap blockage scheme.

3.5 Effects of Aspect Ratio

One of the geometric parameters investigated that appears to have a measurable effect on the scheme is the ratio of the gap height to the thickness of the blade. Figure 19 below compares the effect of three different aspect ratios.

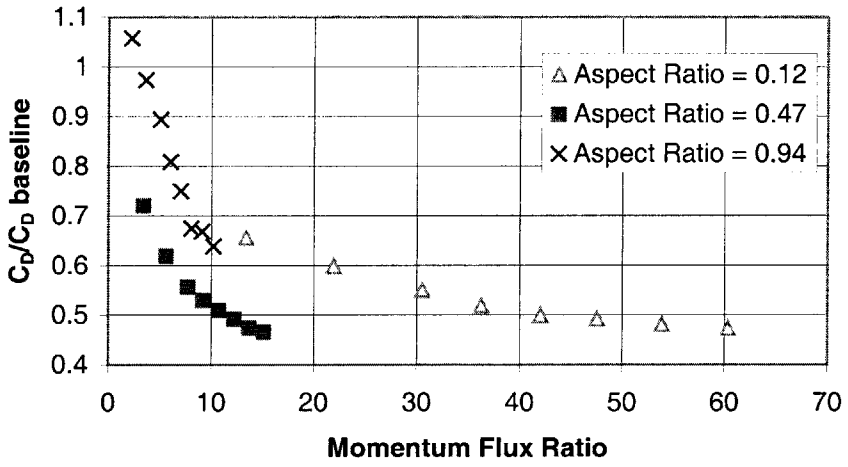

Figure 19. Discharge coefficient ratio vs. momentum flux ratio for three different gap aspect ratios at reduced frequency of 2.0.

In the plot above, all variables are held constant except for the aspect ratio. The reduced frequency is 2.0. While the momentum flux ratios covered for the three cases unfortunately do not coincide exactly, it can be inferred from the data that there is an optimum aspect ratio and that aspect ratio is approximately 0.5. This conclusion is also supported by two other plots: the first, shown below in Figure 20, is a similar plot to Figure 19, but in this figure the data has been gathered at the optimum reduced frequency for each of the cases, whereas Figure 19 occurs at a fixed reduced frequency of 2.0.

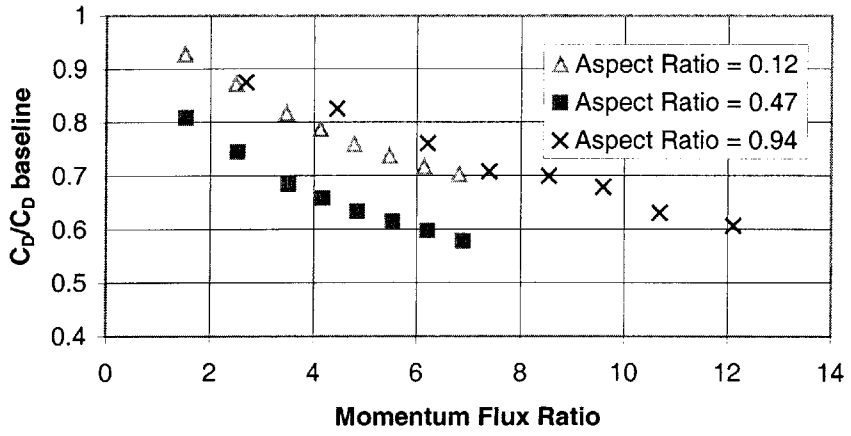

Figure 20. Discharge coefficient ratio vs. momentum flux ratio for three different aspect ratios. These plots were generated at the optimum reduced frequency for each aspect ratio.

The optimum aspect ratio at optimum reduced frequency is the same at 0.47 in the plot above, although the relative effectiveness of the other two aspect ratios is not clear now. The corresponding optimum reduced frequencies for the aspect ratios of 0.12, 0.47 and 0.94 are 0.2, 0.3 and 0.6 respectively.

The other plot, shown below in Figure 21, is a direct plot of the aspect ratio versus the discharge coefficient ratio.

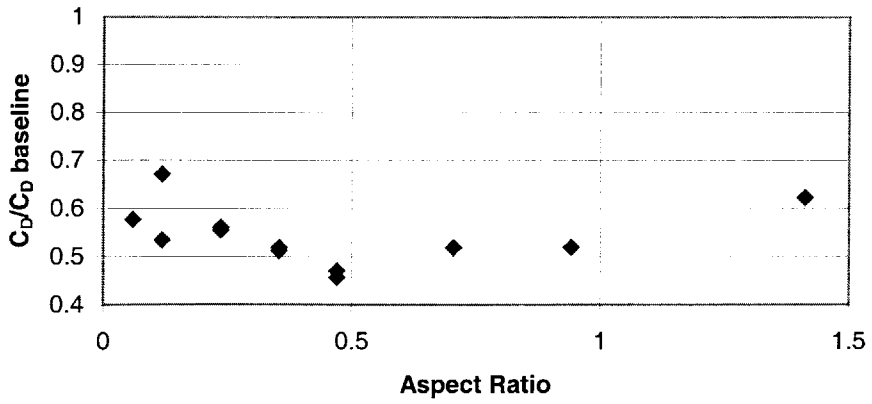

Figure 21. Discharge coefficient ratio vs. aspect ratio at momentum flux of 70.

There are two problems with this plot: firstly, the non-dimensional parameter of orifice exit width over the thickness of the blade is not constant (although it shall soon be shown to be insignificant). Second, the reduced frequency is not held constant in this plot, nor is it set to be the optimum, although the momentum flux ratio is held constant at 70. Even with these caveats, the result is encouraging, not only because it is supported by the above evidence, but also because the plot shows consistent points and trends based on the non-dimensional aspect ratio, even when the physical geometric parameters are varied. The points on the plot that occur at the same non-dimensional aspect ratio correspond to different physical dimensions, and three out of the four places where this occurs coincide. Figures 19, 20 and 21 taken together seem to indicate that there is indeed an optimum aspect ratio, and that that aspect ratio is approximately 0.5.

However, there is no apparent reason why the aspect ratio should have an optimum value. It seems intuitive that the actuator would be more effective as the aspect ratio decreases and becomes small, when the gap height is very small and the plate is very thick. These conditions would make it easier for the synthetic jet to produce an air curtain that extends from the orifice exit to the tip of the plate, and leaving little room for the escape of the leakage flow. Similarly, when the aspect ratio is very high, it would be expected that the jet would be less effective, since it would be more difficult for the jet to provide complete coverage from the orifice exit to the tip of the plate. This is due not only to the increased gap height but also the small tip thickness that the jet sees. This may be, in fact, the trend that is being observed in Figure 21; the experiment is limited in its range by physical parameters, but it appears as if the effectiveness is decreasing as the aspect ratio goes beyond a value of one.

3.6 Effects of Orifice Exit Ratio

The other geometric parameter investigated experimentally is the ratio of the orifice exit width to the thickness of the blade. Due to calibration issues, the physical orifice exit width was not varied, permitting only two variations on the non-dimensional parameter. Figure 22 (identical to Figure 11) below shows the effect of the orifice exit ratio at the respective optimum reduced frequency settings (similar to that described in aspect ratio section) and Figure 23 shows the effect of the orifice exit ratio at a reduced frequency of 2.0.

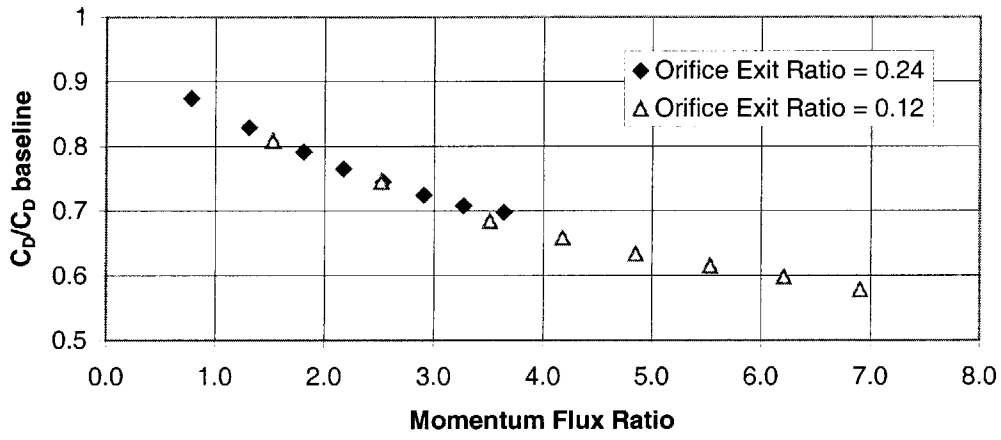

Figure 22. Discharge coefficient ratio vs. momentum flux ratio for two different orifice exit ratios. These experiments were run at their respective optimum reduced frequencies.

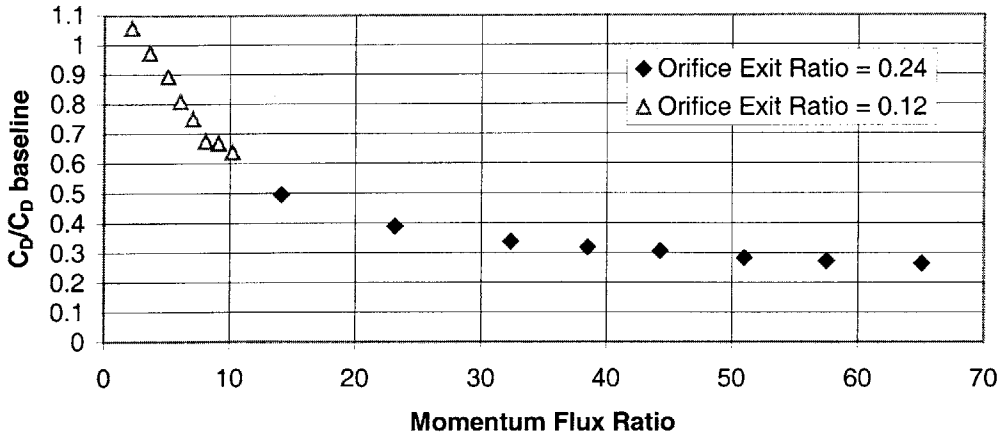

Figure 23. Discharge coefficient ratio vs. momentum flux ratio for two different orifice exit ratios. These experiments were run at a constant reduced frequency of 2.0.

Figure 22 shows the discharge coefficient ratio versus momentum flux ratio for two orifice exit ratios, both of which were tested at their optimum reduced frequencies (which only differ from 0.1 to 0.3 in this case). The curves overlap to a great degree, suggesting no influence on the discharge coefficient by the orifice exit area. Figure 23 shows a similar plot, but at a fixed reduced frequency of 2.0. On this plot, unfortunately, the limitations of the setup did not allow for the curves to overlap, but it certainly appears as if points for the two different cases lie on the same curve.

These plots suggest that the effectiveness of the synthetic jet does not depend on the orifice exit ratio, at least within the narrow limitations of these experiments. It is reasonable that a factor of two in the orifice exit ratio will not have an impact, as long as the momentum flux ratios are held constant. However, it is also reasonable to expect that orifice exit ratios on the order of 1 and higher may result in less effectiveness. Since the momentum flux of the actuator can be altered either by adjusting the velocity of the jet or

the area of the exit, a larger exit area will result in a lower jet velocity for the same jet momentum flux. In the limit of an infinite orifice area, the jet velocity would be zero - resulting in zero-effectiveness. Unfortunately, we cannot see that trend in this experimental setup. Exactly at which orifice ratio the effectiveness begins to decrease is unknown, but it can be inferred that at values of 0.25 or less, the orifice exit ratio does not affect the effectiveness of the actuator in leakage flow blockage.

4.0 Conclusions and Errors

4.1 Conclusions

The most important conclusion to be drawn from this experiment is that significant leakage flow blockage is indeed possible. What is more, a fair amount of control can be exerted over it, depending on the various parameters.

The momentum flux ratio and reduced frequency are the most important parameters. In general, higher momentum flux ratios and lower reduced frequencies will result in improved performance. At the most effective conditions, a reduction in discharge coefficient (and therefore effective gap) of over seventy percent was achieved.

Geometric parameters also play a role, albeit a smaller one. The optimum x-location of the actuator is directly underneath the center of the thickness of the plate. The gap aspect ratio also has an optimum at around 0.5, although the physical reason for it has not yet been cleared up. The orifice exit ratio has no effect on the effectiveness of the scheme, at least within the small scale of ranges that this set of experiments explored.

4.2 Errors and Uncertainties

The largest source of error in the experiment is probably in the hot-wire calibration of the actuator. As mentioned previously, half-profiles had to be taken instead of full profiles. Additionally, the hot-wire itself could not be calibrated at velocities as high as those measured with the hot-wire; in other words, the range of calibration was

exceeded by the range of velocities measured. This was due to the velocity limitations of the wind tunnel in which the hot-wire was calibrated: the maximum wind tunnel velocity was near 30 m/s, whereas the speaker was putting out velocities as high as 45 to 50 m/s. The calibration curve was interpolated to the higher velocities, which is not desirable but was unavoidable. However, as the calibration curve looked reasonable and the interpolation was not far removed from the data points, it is unlikely that the extrapolation of the curve significantly affected the results. A noticeable error in the hot-wire calibration would result in an error in the velocity profile measurement and therefore an error in the momentum flux calibration of the actuator.

Another source of error was the physical setting of the orifice exit and the leakage flow gap. Shim stock was used to ensure consistency in the width of it, but the leakage flow gap had to be blocked off lengthwise near the edges with plasticine so as to make sure the leakage flow was escaping only over the actuator exit. Similarly, plasticine was used to ensure that no portion of the synthetic jet was escaping out of the sides of the actuator exit and not directly out. However, these errors from the physical setup of the experiment are probably minimal.

4.3 Potential Improvements

The major improvement that could be made on this experiment, as alluded to earlier, is the use of a directed synthetic jet at an angle into the oncoming leakage flow. This would not be all that difficult to do, and may result in significantly improved effectiveness. Another option would be to completely detail the effect of the Reynolds

number on the scheme; the schedule of these experiments was not optimized to isolated the Reynolds number as a variable, and again, that should be fairly simple to do.

Beyond that, the next logical step would be to test the concept in a rotating rig. The especially interesting aspect would be to see how the frequency of the rotation affects the result, and the interaction between that frequency, the "frequency" of the leakage flow, and the frequency of the synthetic jet. A rotating rig experiment would flush out the details of the interaction of these frequencies.

Additionally, a cost-benefit type of analysis would be helpful in determining the usefulness of the scheme - whether the increased efficiency is worth the power input and manufacturing costs and such or not. The large reduction in discharge coefficient would suggest that it is worth it (although that depends on the specific application), but a formal analysis would be useful.

4.4 Applicability

With the major improvement in discharge coefficient and virtual gap reduction exhibited with the use of synthetic jet actuation, this concept should be applicable to turbomachinery, at the very least. The major concern is the ability to produce actuators that can generate high momentum fluxes, as the leakage flow velocities and momentum fluxes will be higher than those tested here. However, as demonstrated, the reduced frequency can be controlled to produce good results even at low momentum flux ratios. Ideally, the actuators would be placed on the blade tips themselves, but that is not a

practical solution. Actuators on the casing will be just as effective - the complication comes from the synchronization of the actuators with the blade tips passing by.

The concept can also be used for seals. This will be especially useful if micro-actuators can be fabricated. Of course, the concern again is for generating high enough momentum fluxes, but if the requirement is low than miniature synthetic jets will be a good solution.

Implementation in turbomachinery should not be that difficult and may come about soon. If the power requirements can be met, then there is no reason why this method for improving efficiency cannot be put into practice relatively easily.

Acknowledgements

The author would like to thank a few people for their insight and support. First and foremost, I would like to thank Professor Kenneth Breuer, my supervisor. In addition, I would like to acknowledge Professor Ed Greitzer, Dr. Choon Tan, Jinwoo Bae, and Huu Duc Vo for their weekly input. Last but not least, I would like to thank the support staff of the Gas Turbine Laboratory - especially Viktor Dubrowski and James Letendre.

Bibliography

1. Smith, B.L. and Glezer, A. "The formation and evolution of synthetic jets." *Physics of Fluids*, Vol. 10, No. 9, September 1998, pp. 2281-2297.

2. Ingard, U. "On the Theory and Design of Acoustic Resonators." *The Journal of the Acoustical Society of America*, Vol. 25, No. 6, November 1953, pp. 1037-1060.

3. Abramovich, G.N. The Theory of Turbulent Jets. MIT Press, Cambridge MA, 1963.

4. Idel'Chik, I.E. Handbook of Hydraulic Resistance. Israel Program for Scientific Translations Ltd., Jerusalem, 1966.

5. Rathnasingham, R. and Breuer, K.S. "Coupled Fluid-Structural Characteristics of Actuators for Flow Control." *AIAA Journal*, Vol. 35 (5), May 1997, pp. 832-837.

6. Roy, R. A Primer on the Taguchi Method. Van Nostrand Reinhold, New York, 1990.